J. Biochem. 2016;159(4):471–479 doi:10.1093/jb/mvv118

JB THE JOURNAL OF BIOCHEMISTRY

Effects of the N terminus of mouse DNA polymerase κ on the bypass of a guanine-benzo[a]pyrenyl adduct

Received July 13, 2015; accepted November 14, 2015; published online December 3, 2015

Yang Liu*, Xiaolu Ma and Caixia Guo†

Key Laboratory of Genomic and Precision Medicine, China Gastrointestinal Cancer Research Center, Beijing Institute of Genomics, Chinese Academy of Sciences, Beijing 100101, China

*Yang Liu, Key Laboratory of Genomic and Precision Medicine, China Gastrointestinal Cancer Research Center, Beijing Institute of Genomics, Chinese Academy of Sciences, No.1 Beichen West Road, Chaoyang District, Beijing 100101, China. Tel: 010-86-84097678, email: liuyang@big.ac.cn

†Caixia Guo, Key Laboratory of Genomic and Precision Medicine, China Gastrointestinal Cancer Research Center, Beijing Institute of Genomics, Chinese Academy of Sciences, No.1 Beichen West Road, Chaoyang District, Beijing 100101, China. Tel: 010-86-84097646, email: guocx@big.ac.cn

DNA polymerase κ (Polκ), one of the typical member of the Y-family DNA polymerases, has been demonstrated to bypass the 10*S* (+)-*trans*-*anti*-benzo[*a*]pyrene diol epoxide-N^2-deoxyguanine adducts (BPDE-dG) efficiently and accurately. A large structural gap between the core and little finger as well as an N-clasp domain are essential to its unique translesion capability. However, whether the extreme N-terminus of Polκ is required for its activity is unclear. In this work, we constructed two mouse Polκ deletions, which have either a catalytic core (mPolκ$_{1\text{-}516}$) or a core without the first 21-residues (mPolκ$_{22\text{-}516}$), and tested their activities in the replication of normal and BPDE-DNA. These two Polκ deletions are nearly as efficient as the full length protein (Polκ$_{1\text{-}852}$) in normal DNA synthesis. However, steady-state kinetics reveals a significant reduction in efficiency of dCTP incorporation opposite the lesion by Polκ$_{22\text{-}516}$, along with increased frequencies for misinsertion compared with Polκ$_{1\text{-}852}$. The next nucleotide insertion opposite the template C immediately following the BPDE-dG was also examined, and the bypass differences induced by deletions were highlighted in both insertion and extension step. We conclude that the extreme N-terminal part of Polκ is required for the processivity and fidelity of Polκ during translesion synthesis of BPDE-dG lesions.

Keywords: translesion DNA synthesis/Y-family DNA polymerase κ/polycyclic aromatic hydrocarbons/BPDE-dG lesions/enzyme fidelity.

The human genome is exposed to a variety of endogenous and exogenous stresses that lead to DNA damages. Although most damaged DNAs are efficiently repaired by cellular repair system, those that escape repair strongly affect DNA replication in the S phase. Translesion DNA synthesis (TLS) is one of the DNA damage tolerance processes. It employs specialized TLS polymerases to synthesize DNA across and beyond a variety of replication-blocking lesions, thus avoiding replication fork collapse (*1*). Up to date, eight translesion synthesis polymerases have been identified in mammals, and four of them, namely Polη, Polι, Polκ and REV1 belong to the Y-family (*2–4*).

Due to the different nature and structure of DNA adducts, every Y-family member exhibits distinct preference for specific DNA lesions (*5*). For example, the eukaryotic Polη is specialized in accurately bypassing cyclobutane pyrimidine dimer (CPD) with insertion of two dATP opposite a TT dimer (*6*, *7*). Crystal structure studies show that Polη functions as molecular splint to stabilize the TT dimer in a normal B-form conformation, and the CPD lesion is well accommodated in the active site for translesion synthesis (*8*). Deficiency of Polη leads to a variant form of xeroderma pigmentosum diseases (*9*, *10*). Although Polι could not replicate the TT dimer (*11*), it has been suggested to be involved in the error free (*12*) or error prone (*13*) replication of certain N^2-deoxyguanine (dG) adducts, such as 1,N^2-propano-2′deoxyguanosine (γ-HOPdG) resulting from lipid peroxidation or N^2-dG adducts derived from 2-amino-3-methylimidazo[4,5-f]quinoline, respectively. Recently, based on reported germline variations in human Single Nucleotide Polymorphism database, several genetic variants of Polι have been constructed and their biochemical activities of bypassing different lesions, such as abasic site, 8-oxoG, O^6-MeG and N^2-EtG lesion, have been examined (*14*). These data suggest that certain genetic variations in the TLS polymerases affect their nucleotide incorporation *in vitro* (*14*). REV1, which is unable to support TLS across TT dimers or [6-4] photoproducts, acts as scaffold protein and plays roles in regulating other TLS polymerases' activities (*15*). Polκ, the only Y family member with homologs in both bacteria (Dinb and Pol IV) and archaea (Dpo4 and Dbh), is most ubiquitous among eukaryotic Y-family polymerases.

A classic polymerase catalytic core consisting of palm, thumb and finger domains and an additional little finger (LF) domain are present in all Y-family polymerases. A N-clasp subdomain, which covers residues 21-74 and augments the conventional right-handed grip on the primer-template by the palm, fingers and thumb domains is observed in Polκ (*16*). The catalytic core of human apo Polκ with the first 18-67-residue removed (19-526 and 68-526 aa) have been studied by X-ray crystallography either alone (*16*) or in complex with a normal template-primer and an incoming nucleotide (*17*). Although residues 19-32 are disordered in the crystal structure, residues 33-74 encircle a normal primer/template pair (*17*) and residues 19-68

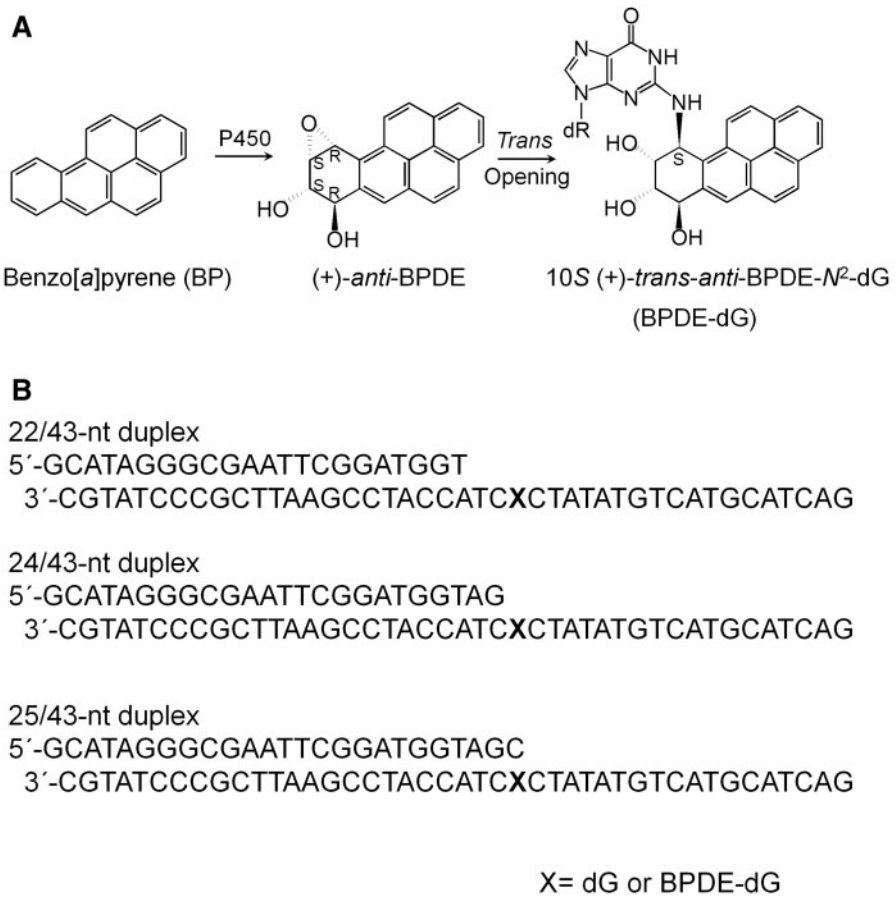

Fig. 1 (A) Structures of benzo[*a*]pyrene (BP), its metabolite (+)-(7*R*,8*S*,9*S*,10*R*) diol epoxide (+)-*anti*-BPDE) and the 10*S* (+)-*trans-anti*-BPDE-N^2-dG (10*S* (+)-*trans-anti*-[BP]-N^2-dG) adduct. **(B)**. Sequence context employed in the assay. The running-start assay was done by 22/43-nt duplex, and the standing-start experiment for single nucleotide incorporation opposite the G (or BPDE-dG adduct) and the template base C immediately following the G (or BPDE-dG adduct) is done by 24/43-nt and 25/43-nt duplexes, respectively.

is required for DNA synthesis from matched and mismatched primer-template termini (*17*). Human Polκ (hPolκ) with removal of either the first 67-aa (68-526) or 90-residue (91-559) has attenuated catalytic activity over mismatched primer termini compared with the catalytic core (1-526) or the core minus the first 18 residues (19-526) (*16*, *17*). At present, whether residues 1-18 of the extreme N-terminus of hPolκ are required for its TLS function remain unclear.

(+)-7R,8S,9S,10R- benzo[*a*]pyrene dihydrodiol epoxide [(+)-*anti*-BPDE] is the most mutagenic and tumorigenic metabolite of benzo[*a*]pyrene (B[*a*]P) (Fig. 1A), the representative member of polycyclic aromatic hydrocarbons (PAHs) that is present in polluted air and in tobacco smoke (*18*). (+)-*anti*-BPDE reacts readily with the exocyclic amino groups of guanine residues in DNA forming the major (+)-*trans-anti*-BPDE-N^2-dG adducts (abbreviated as BPDE-dG) (Fig. 1A) (*19*). Several *in vivo* and/or *in vitro* studies have identified that BPDE-dG adduct might among the cognate or the most preferred lesion substrates for Polκ. Polκ can perform error-free bypass of the bulky minor groove (+)-BPDE-dG adduct with incorporating correct dCTP opposite the lesion (*20*–*22*). The uniquely large structural gap between the core and LF domain in Polκ is demonstrated to be essential for accommodating minor groove (+)-BPDE-dG adduct and for efficient bypass (*23*). mPolκ with the first 51 residues deleted (52-516) leads to failure of BPDE bypass but not for normal DNA synthesis (*23*). In correspondence to *in vitro* analyses, Polκ-deficient mouse embryo fibroblasts and embryo stem cells are sensitive to benzo[*a*]pyrene treatment and exhibit increased BPDE-induced mutagenesis (*24*–*27*).

In this study, we analysed whether the extreme N-terminus of mPolκ (1-21), which is equivalent to residues 1-22 in hPolκ, is required for Polκ in processing of the bulky minor groove BPDE-adduct. To answer that, we constructed $Polκ_{1\text{-}516}$ and $Polκ_{22\text{-}516}$ (Fig. 2A) and compared their ability to replicate DNA opposite BPDE modified dG as well as undamaged DNAs. Our results reveal that the extreme N-terminal part of Polκ is required for its bypass of BPDE-dG lesions, and both the replication fidelity and the processivity are greatly affected by the modifications.

Experimental Procedures

Materials

All chemicals were analytical grade. The enzyme OptiKinase was obtained from USB Molecular Biology Reagents and Biochemicals (Cleveland, OH). The T4 DNA ligase was obtained from New

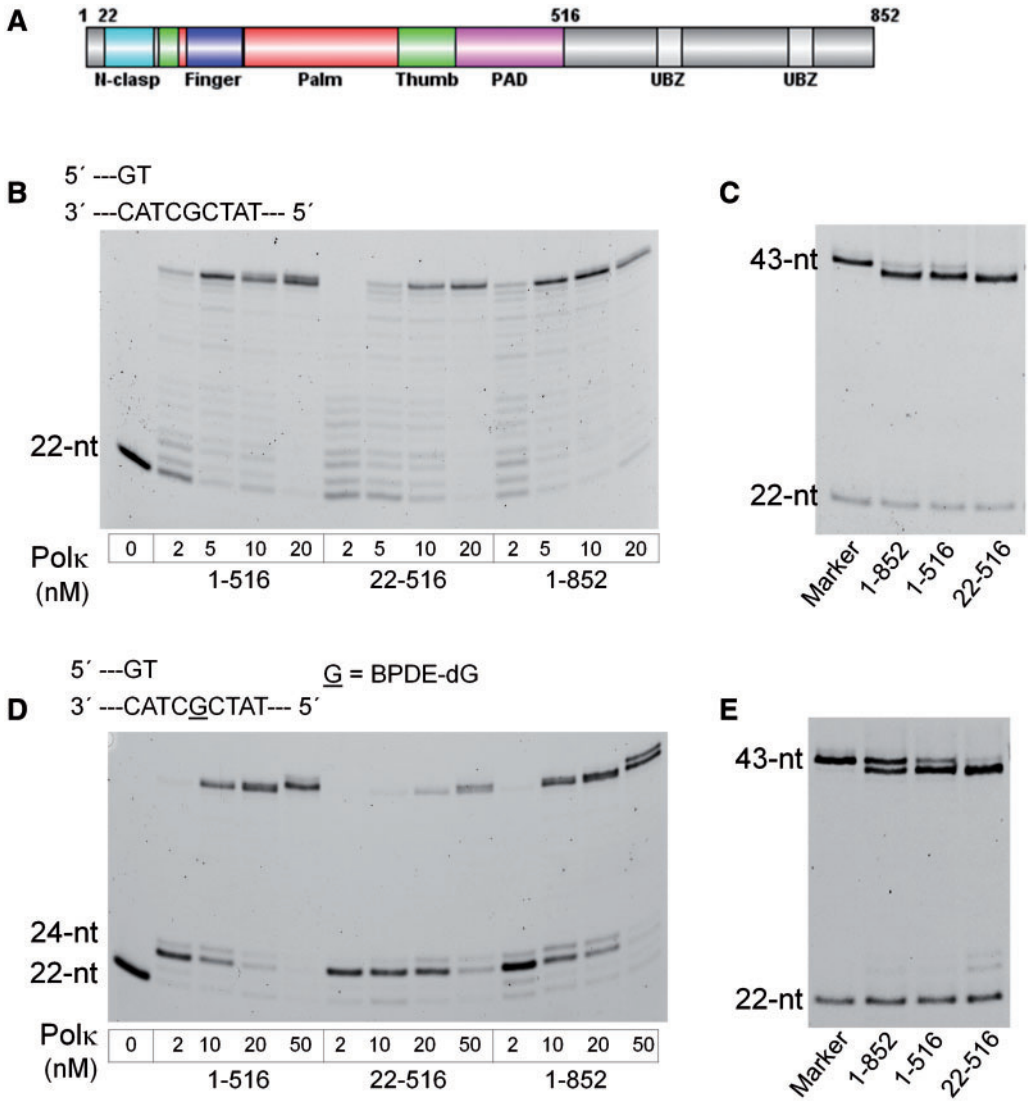

Fig. 2 Primer extension opposite normal and (+)-*trans*-*anti*-BPDE-N^2-dG templates by the full-length and truncated mPolκ. (A) The structure domains of mPolκ. The schematic diagram is drawn by DOG (v.2.0) (*38*), with truncation sites indicated. **(B)** Running-start primer extension experiments on normal DNA template. Reactions were carried out in the presence of all four dNTPs for 5 min at 37°C with increased concentrations of Polκ as shown below each track. **(C)** Analysis of extension product lengths over normal dG template by full-length and truncated mPolκ. 43-nt marker sequence as well as 22-nt primer is in a separate lane. The sequence context of the 43-nt marker, which corresponds to the primer full extension product strand in Figure 1B, is listed in the 'Materials' section. The reactions were catalysed by 20 nM Polκ at 37°C for 10 min. **(D)** Running-start primer extension experiments on BPDE-dG template. Reactions were carried out with increasing concentrations of Polκ at 37°C for 10 min. The underlined G represents the BPDE-dG lesion. The 22-nt primer was readily extended to the two nucleotides 3′ of the lesion and stalled at template position 24-nt, immediately before the lesion. **(E)** Comparison of primer extension products length catalysed by full-length and truncated mPolκ using the BPDE-dG template. The assays included 50 nM of each Polκ at 37°C for 20 min.

England BioLabs (Ipswich, MA). The dNTPs were also purchased from NEB. The 5′ 6-carboxyfluorescein (6-FAM)-labelled 22-nt primer 5′-GCATAGGGCGAATTCGGATGGT-3′, 24-nt primer 5′-GCATAGGGCGAATTCGGATGGTAG-3′ and 25-nt primer 5′-GCATAGGGCGAATTCGGATGGTAGC-3′ (Fig. 1B) were purchased from Life Technologies (Shanghai, China). The 5′ 6-carboxyfluorescein (6-FAM)-labelled 43-nt marker sequence 5′-GCATAGGGCGAATTCGGATGGTAGCGATATACAGTACGTAGTC-3′ was purchased from Generay BioTechnologies (Shanghai, China). The unmodified oligonucleotides were obtained from Sangon, Inc. (Shanghai, China). The oligonucleotides were further purified by 20% denaturing polyacrylamide gel electrophoresis (PAGE) containing 7.5 M Urea. The (+)-*trans*-BPDE-dG lesion embedded in 11-nt sequence 5′-ATATCGCTACC-3′ (the underlined G represents the BPDE- dG lesion) is generated as previously described (*28*). The 11-nt sequence is further ligated to the left 13-nt (5′-GACTACGTACTGT-3′) and right 19-nt (5′-ATCCGAATTCGCCCTATGC-3′) forming the final 43-nt products in the context of (5′-GACTACGTACTGTATATCGCTACCATCCGAATTCGCCCTATGC-3′) (Fig. 1B).

Purification of the full length and truncated mPolκ proteins

Full-length mPolκ-pET-16b expression vector was constructed as described previously (*29*). The catalytic core mPolκ$_{1\text{-}516}$ and N-terminal truncated mPolκ$_{22\text{-}516}$ constructs were generated by PCR amplification. Each construct was sequenced correctly. The proteins were expressed and purified as described in (*23*).

Running-start primer extension assay by the full-length and truncated mPolκ in vitro

For *in vitro* primer extension experiments, the unlabelled and the 5′- end labelled 6-FAM-primer 22-nt 5′-GCATAGGGCGAATTCGGATGGT-3′ were annealed to the template strand 5′-GACTACGTACTGTATATCXCTACCATCCGAATTCGCCCTATGC-3′ at a molar ratio of 1:1.2, where X is dG or BPDE-dG. The newly

Table I. Steady-state kinetic parameters for nucleotide incorporation opposite the normal G template by the full length and truncated mPolκ proteins

Polκ	dNTP	k_{cat} (min^{-1})	K_m (μM)	k_{cat}/K_m (min^{-1} μM^{-1})	f_{ins}[a]	Relative efficiency[b]
	A	0.29 ± 0.013	91.5 ± 20	3.2×10^{-3}	7.9×10^{-4}	
1-852	C	11.5 ± 2.5	2.86 ± 1.2	4	1	1
	T	0.43 ± 0.018	36.7 ± 7.9	1.2×10^{-2}	2.8×10^{-3}	
	G	2.68 ± 0.3	311 ± 21	8.6×10^{-3}	2.1×10^{-3}	
	A	1.11 ± 0.04	210 ± 8.9	5.3×10^{-3}	8.2×10^{-4}	
1-516	C	14.9 ± 0.25	2.31 ± 0.34	6.4	1	1.6
	T	0.71 ± 0.11	14.4 ± 4.6	4.9×10^{-2}	7.6×10^{-3}	
	G	2.05 ± 0.7	170 ± 12	1.2×10^{-2}	1.9×10^{-3}	
	A	0.73 ± 0.16	4354 ± 465	1.7×10^{-4}	3.8×10^{-5}	
22-516	C	13.7 ± 2.0	3.10 ± 1.5	4.4	1	1.1
	T	0.35 ± 0.06	41.8 ± 11	8.4×10^{-3}	1.8×10^{-3}	
	G	0.39 ± 0.12	2574 ± 482	1.5×10^{-4}	3.4×10^{-5}	

[a]Misinsertion frequency, calculated by dividing k_{cat}/K_m for each single dNTP incorporation by the k_{cat}/K_m for dCTP incorporation opposite undamaged G. [b]Relative efficiency, calculated by dividing k_{cat}/K_m of truncated Polκ$_{1\text{-}516}$ or Polκ$_{22\text{-}516}$ for dCTP incorporation opposite normal G by that of k_{cat}/K_m of the full length Polκ$_{1\text{-}852}$.

prepared enzyme (0–50 nM) was mixed with 0.2 μM unlabelled and 20 nM corresponding 6-FAM 5′-end labelled primer/template duplexes in the solution containing 25 mM Tris-HCl (pH 7.0), 0.1 mg/ml BSA, 1 mM DTT, 5 mM $MgCl_2$, 5 mM NaCl and 2.5% (wt/vol) glycerol. The reaction is preincubated at 37°C for 10 min and after initiation by the addition of dNTP mixture (*30*), the reaction was allowed to proceed at 37°C for indicated time slots. Products were terminated with 5 μl stop solution containing 20 mM EDTA, 95% formamide, 0.05% bromophenol blue and 0.05% xylene cyanol. After heating to 95°C for 3 min, the extension products were separated on 15% denaturing polyacrylamide (w/v) gel, and quantified using Typhoon 9500 (GE Healthcare) and Image Quant version 5.2 (Amersham Biosciences).

Steady-state kinetic analyses

For the steady-state kinetic analysis, the 6-FAM labelled 24-nt primer 5′-GCATAGGGCGAATTCGGATGGTAG-3′ was annealed with the unmodified or BPDE-modified 43-nt template at a primer/template ratio of 1:1.2, resulting the 24/43-nt duplex. The 3′ end of primer pairs with the template base 3′ preceding the adduct, and a single nucleotide insertion opposite the lesion was determined according to previously published methods (*31–33*). To examine extension from G or BPDE-dG paired with C template: primer termini, the 6-FAM labelled 25-nt primer 5′-GCATAGGG CGAATTCGGATGGTAGC-3′ was annealed with the corresponding 43-nt template forming the 25/43-nt duplex, and the kinetic parameters were determined for single dNTP incorporation opposite the template base C immediately following the G or the BPDE-dG adduct. The polymerase concentrations 2–20 nM enzyme(s), variable concentrations of a single nucleotide and reaction times 2, 5 or 10 min were selected to ensure that the maximal product formation was <20% (*32*, *34*). The reactions were terminated, subjected to denaturing PAGE and analysed using the Typhoon 9500. The parameters k_{cat} and K_m were extracted from the nonlinear regression fit of the Michaelis-Menten equation using Origin 8.0 software. All experiments were carried out in triplicate. Error bars indicate the standard deviation. The insertion efficiencies is indicated by k_{cat}/K_m, and the misincorporation frequency (f) is calculated from the expression $f_{ins} = (k_{cat}/K_m)_{dNTP}/(k_{cat}/K_m)_{dCTP}$.

Results

Primer extension assays by the full-length and truncated mPolκ proteins

Full-length and both truncated Polκ proteins (Polκ$_{1\text{-}516}$ and Polκ$_{22\text{-}516}$) were purified to near homogeneity using FPLC as previously reported (*23*) (Supplementary Fig. S1). Though at low enzyme concentration of 2 nM, Polκ$_{22\text{-}516}$ exhibited less activity compared with Polκ$_{1\text{-}852}$ and Polκ$_{1\text{-}516}$, it readily extended the primer to the end of the normal DNA template at enzyme concentrations above 2 nM, as that of the other two proteins (Fig. 2B). A dominant 42-nt product in addition to a minor 43-nt was observed for Polκ$_{1\text{-}852}$ and Polκ$_{1\text{-}516}$, while Polκ$_{22\text{-}516}$ exhibited extended 42-nt product only (Fig. 2C).

The presences of a BPDE-dG adduct retarded primer extension catalysed by different Polκ. Full length and both truncated Polκ extended the 22-nt primer by two nucleotides and paused immediately before the adduct at 24-nt (Fig. 2D). However, primer stalling of Polκ$_{22\text{-}516}$ is highly pronounced compared with Polκ$_{1\text{-}852}$ and Polκ$_{1\text{-}516}$ proteins. When the polymerase concentration was increased from 2 to 50 nM, eventually all primers were extended to the end or near the end of the template strand by the full length and truncated Polκ$_{1\text{-}516}$ protein (Fig. 2D), while Polκ$_{22\text{-}516}$ displayed limited replication ability across the adduct. These data suggested that lack of the first 21-aa leads to the inefficient lesion bypass by Polκ$_{22\text{-}516}$. However, Polκ$_{22\text{-}516}$ could extend the primer to the end when increasing the enzyme concentration and the extension product is in proportion to enzyme concentration. In addition, extension product length varied with different Polκ forms. Polκ$_{1\text{-}852}$ and Polκ$_{1\text{-}516}$ generated 42- and 43-nt extension products; and Polκ$_{22\text{-}516}$ predominantly produced 42- and a little 43-nt (Fig. 2E).

Steady-state kinetic measurements of the full-length and Polκ truncations

Kinetic parameters k_{cat} and K_m were measured first with the full length and truncated Polκ proteins for single dNTP insertion opposite normal G template (Table I), and the examples of typical single dCTP insertion assays were depicted in Figure 3A. Polκ$_{1\text{-}516}$ behaved like Polκ$_{1\text{-}852}$ on native DNA, and both are accurate in dCTP incorporation opposite G, with misincorporation frequencies $[(k_{cat}/K_m)_{incor}/(k_{cat}/K_m)_{cor}]$ in the order of 10^{-3} to 10^{-4} (Table I). When compared with Polκ$_{1\text{-}516}$ and Polκ$_{1\text{-}852}$, Polκ$_{22\text{-}516}$ displayed higher accuracy in incorporating single dCTP opposite undamaged G, with misincorporation frequencies in

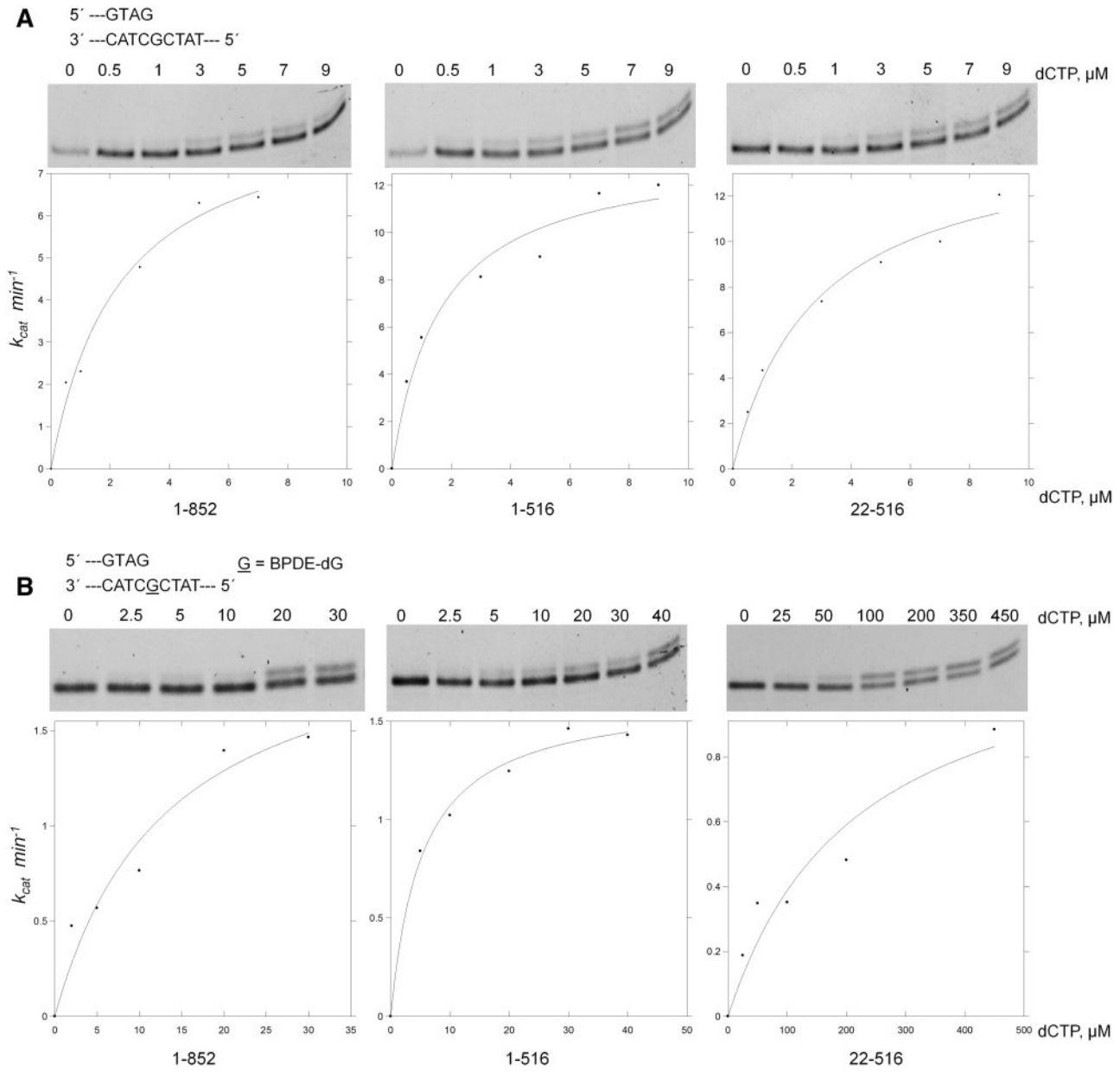

Fig. 3 Kinetics of single nucleotide insertion opposite (A) undamaged G or (B) BPDE-dG template by full length and truncated mPolκ. The gels (top panels) and plot (bottom panels) show data as a function of dCTP concentration. 0.2 μM unlabelled and 20 nM corresponding 6-FAM 5′-end labelled primer/template duplexes was incubated with 2 nM Polκ$_{1\text{-}852}$, Polκ$_{1\text{-}516}$ or Polκ$_{22\text{-}516}$ in the presence of dCTP for 2 min under the normal strand **(A)** or was incubated with 10 nM Polκ$_{1\text{-}852}$, Polκ$_{1\text{-}516}$ or Polκ$_{22\text{-}516}$ in the presence of dCTP for 5 min at 37°C on the BPDE modified strand **(B)**. The primer extension data recorded (with <20% of primer extended) were used for estimation of Michaelis-Menten parameters listed in Tables I and II. Extended primers were separated by 15% denaturing PAGE. Variants of mPolκ mediated kinetics of single nucleotide incorporation on G or BPDE-dG by dATP, dTTP or dGTP were listed in Supplementary Figure S2.

the order of 10^{-3} to 10^{-5} (Table I). The greater reduction of misinsertion efficiencies (k_{cat}/K_m) of dATP and dGTP of Polκ$_{22\text{-}516}$ stems from increased K_m compared with those of Polκ$_{1\text{-}516}$ and Polκ$_{1\text{-}852}$, which suggested that the first 21 residues contribute additionally to the misinsertion efficiency while the catalytic efficiencies for correct nucleotide incorporation opposite unmodified template G are similar among different Polκ forms (Table I).

k_{cat} and K_m were also determined for the full-length and truncated Polκ with respect to nucleotide insertion opposite the (+)-BPDE-dG adduct (Table II), and the representative single dCTP insertion experiments were shown in Figure 3B. When compared with Polκ$_{1\text{-}852}$, Polκ$_{22\text{-}516}$ catalytic core led to a decrease in the efficiency of dCTP insertion opposite a damaged G (k_{cat}/K_m) by 28-fold (Table II), which is consistent with the observation that Polκ$_{22\text{-}516}$ is more severely blocked by BPDE-dG than Polκ$_{1\text{-}852}$ in the running-start primer extension assay (Fig. 2D). On the other hand, Polκ$_{1\text{-}516}$ exhibits 1.7-fold increase in dCTP insertion efficiency relative to that of the full length Polκ (Table II).

The single dNTP insertion across the BPDE-dG lesion by Polκ$_{1\text{-}852}$ and both truncated Polκ is accurate (Table II), the misinsertion frequencies of dATP and dTTP are decreased by two or three orders of

Table II. Steady-state kinetic parameters for nucleotide incorporation opposite the (+)-*trans-anti*-BPDE-N^2-dG adduct by the full length and truncated mPolκ proteins[a,b]

Polκ	dNTP	k_{cat} (min^{-1})	K_m (μM)	k_{cat}/K_m (min^{-1} μM^{-1})	f_{ins}[c]	Relative efficiency[d]
	A	0.42 ± 0.06	326 ± 75.3	1.3×10^{-3}	8.5×10^{-3}	
1-852	C	2.42 ± 0.04	16.0 ± 3.54	1.5×10^{-1}	1	3.8×10^{-2}
	T	0.35 ± 0.01	623 ± 190	5.6×10^{-4}	3.6×10^{-3}	
	A	0.36 ± 0.11	103 ± 6.05	3.5×10^{-3}	1.3×10^{-2}	
1-516	C	1.64 ± 0.24	6.35 ± 1.42	2.6×10^{-1}	1	6.5×10^{-2}
	T	0.35 ± 0.05	606 ± 91.5	5.8×10^{-4}	2.2×10^{-3}	
	A	0.11 ± 0.03	432 ± 38.0	2.5×10^{-4}	4.6×10^{-2}	
22-516	C	1.14 ± 0.35	210 ± 62.7	5.4×10^{-3}	1	1.4×10^{-3}
	T	0.18 ± 0.04	1906 ± 285	9.4×10^{-5}	1.7×10^{-2}	

[a]A 24/43-nt duplex (sequence indicated in Fig. 1B) was used in the assay. [b]No apparent incorporation of dGTP was observed even when high concentration of 2.5 mM dNTP was used by the full length and the deletions. Thus, steady-state kinetic parameters were determined only for dA, dC and dTTP incorporation. [c]Misinsertion frequency, calculated by dividing k_{cat}/K_m for each single dNTP incorporation by the k_{cat}/K_m for dCTP incorporation opposite BPDE-dG. [d]Relative efficiency, calculated by dividing k_{cat}/K_m of Polκ$_{1\text{-}852}$, truncated Polκ$_{1\text{-}516}$ or Polκ$_{22\text{-}516}$ for dCTP incorporation opposite BPDE-dG adduct by that of k_{cat}/K_m of the full length Polκ$_{1\text{-}852}$ for dCTP insertion opposite normal G in Table I.

Table III. Steady-state kinetic parameters for correct nucleotide dGTP incorporation opposite template base C immediately following G or BPDE-dG adduct by full-length, 1-516, and 22-516 mPolκ[a]

Normal G template, 25/43-nt duplex				
Polκ	**k_{cat} (min^{-1})**	**K_m (μM)**	**k_{cat}/K_m (min^{-1} μM^{-1})**	**Relative to Polκ $_{1\text{-}852}$[b]**
1-852	3.45 ± 0.20	0.684 ± 0.150	5.0	1
1-516	7.35 ± 1.44	0.948 ± 0.737	7.8	1.6
22-516	1.16 ± 0.11	0.912 ± 0.284	1.3	2.6×10^{-1}
BPDE-dG template, 25/43-nt duplex				
Polκ	**k_{cat} (min^{-1})**	**K_m (μM)**	**k_{cat}/K_m (min^{-1} μM^{-1})**	**Relative to Polκ $_{1\text{-}852}$[c]**
1-852	2.03 ± 0.11	10.6 ± 2.36	1.9×10^{-1}	3.8×10^{-2}
1-516	2.24 ± 0.41	3.62 ± 0.57	6.2×10^{-1}	1.2×10^{-1}
22-516	1.01 ± 0.25	39.2 ± 0.50	2.6×10^{-2}	5.2×10^{-3}

[a]A 25/43-nt duplex (sequence indicated in Fig. 1B) was used in the assay. [b]Relative efficiency, calculated by dividing k_{cat}/K_m of truncated Polκ$_{1\text{-}516}$ or Polκ$_{22\text{-}516}$ for dGTP incorporation opposite template C immediately following normal G by that of k_{cat}/K_m of the full length Polκ$_{1\text{-}852}$. [c]Relative efficiency, calculated by dividing k_{cat}/K_m of Polκ$_{1\text{-}852}$, truncated Polκ$_{1\text{-}516}$ or Polκ$_{22\text{-}516}$ for dGTP incorporation opposite template C immediately following BPDE-dG adduct by that of k_{cat}/K_m of the full length Polκ$_{1\text{-}852}$ for dGTP insertion opposite template C from the undamaged G:C pair.

magnitude, respectively, compared with that of dCTP incorporation (Table II). An increased K_m compared with dCTP incorporation contributes to the decreased efficiencies of dATP or dTTP misinsertion by Polκ$_{1\text{-}852}$ and Polκ$_{1\text{-}516}$. Polκ$_{22\text{-}516}$ shows reduced fidelity compared with Polκ$_{1\text{-}852}$ and Polκ$_{1\text{-}516}$ (Table II). Notably, though both Polκ truncations and Polκ$_{1\text{-}852}$ prefer to misincorporate dATP, Polκ$_{22\text{-}516}$ exhibits increased frequency for dTTP misinsertion opposite BPDE-dG compared with that of the Polκ$_{1\text{-}852}$ and Polκ$_{1\text{-}516}$ by 5- and 8-fold, respectively (Table II).

Extension by a single nucleotide beyond the undamaged and the BPDE-adducted G with both the full length and truncated mPolκ

In order to determine whether different primer extension patterns are present in the step immediately following dCTP insertion, we set out to measure the steady-state kinetics of base extension efficiency beyond the undamaged and BPDE damaged-dG. The kinetic parameters were determined for the next base extension from G: C or BPDE-dG: C pair of 25/43-nt duplex with different Polκ forms (Table III). In the case of the next base extension from normal G: C template: primer pair termini, both the full length and truncated Polκ$_{1\text{-}516}$ protein showed similar pattern to the correct nucleotide incorporation opposite undamaged G (Table I). Notably, the efficiency of dGTP insertion opposite template C immediately following the undamaged G by Polκ$_{22\text{-}516}$ is reduced by 4-fold compared with that of the Polκ$_{1\text{-}852}$ (Table III).

In addition, the kinetic parameters have also been measured for dGTP insertion opposite template C immediately following BPDE-dG (Table III). Polκ$_{22\text{-}516}$ exhibits the lowest catalytic capability of dGTP incorporation compared with that of Polκ$_{1\text{-}852}$ and Polκ$_{1\text{-}516}$, as expected from both primer extension result (Fig. 2D) and steady-state kinetics of nucleotide insertion opposite the lesion (Table II). Together, these results suggest that deletion of the first 21 residues in Polκ impairs both insertion and the subsequent extension step beyond the adduct.

Discussion

The N-clasp, although seemingly dispensable for normal DNA synthesis and being structurally disordered (*16*, *17*), plays critical roles in Polκ's polymerase activity. In this study, we examined whether the extreme N-terminal 21 residues in mPolκ, closely adjacent to the N-clasp, are required for its bypass of BPDE-dG lesions. Two truncated forms, Polκ$_{1\text{-}516}$ and Polκ$_{22\text{-}516}$ were generated. We found that Polκ$_{22\text{-}516}$ manifested an impaired TLS activity in bypass of the BPDE-DNA template and the deleted 21 residues contribute to the BPDE bypass efficiencies and subsequent extension proficiency.

Studies using the *in vitro* primer extension assay reveal that both Polκ$_{1\text{-}516}$ and Polκ$_{22\text{-}516}$ retain activities comparable to Polκ$_{1\text{-}852}$ on normal DNA (Fig. 2B). Steady-state analyses indicate similar dCTP incorporation efficiencies among different Polκ forms (Table I), which suggests that the first 21 residues are not necessary for normal DNA synthesis. When comparing the steady-state kinetic parameters for nucleotide extension from G:C pair template: primer termini using 25/43-nt duplex, we found Polκ$_{22\text{-}516}$ extends the primer less efficiently than Polκ$_{1\text{-}516}$ or Polκ$_{1\text{-}852}$ (Table III), suggesting that the reduced frequency of Polκ$_{22\text{-}516}$ for the next base extension beyond the undamaged G might explain its less activity under low concentration in running start primer extension assays as shown in Figure 2B. Anyway, the reduction could be complemented by increasing the enzyme concentration (Fig. 2B). Additionally, removal of the extreme N-terminal 21 residues of mPolκ leads to a reduction in the misincorporation efficiencies of dATP or dGTP opposite undamaged G (Table I), suggesting that the deletion influences the ability of Polκ to discriminate purines during incorporation opposite the unmodified G.

Under the BPDE damaged template, Polκ$_{22\text{-}516}$ manifests a strongly impaired TLS ability, leading to primer pausing in the vicinity of the adduct, while Polκ$_{1\text{-}516}$ exhibits a higher TLS ability compared with that of the full length mPolκ (Fig. 2D). The data indicate that the first 21 residues in mPolκ are required for its optimal bypass of BPDE-dG lesion. The differences in polymerase stalling due to amino acid deletions are mirrored in the different catalytic efficiencies of dCTP incorporation opposite BPDE-dG (Table II), in next base extension immediately following the adduct (Table III) and in the overall TLS efficiencies (Supplementary Fig. S3) calculated by multiplying the relative efficiency for dCTP insertion opposite G (or BPDE-G) (Tables I and II) and the relative efficiency for the next base extension (Table III) by different Polκ as described previously (*35*, *36*). When removal of the 1-21aa of Polκ catalytic core, we see a 28-fold decreases in correct dCTP incorporation efficiency opposite the BPDE-dG adduct compared with that of Polκ$_{1\text{-}852}$, with the increase in K_m largely in charge of the reduction (Table II). Polκ$_{22\text{-}516}$ also showed a 7-fold decrease in k_{cat}/K_m for next base extension from the G*: C pair termini compared with that with the full length mPolκ (Table III), suggesting that deletion influences Polκ's activity for next base extension from both G: C and G*: C pairs (Table III). The preference for misincorporating dATP is pronounced by both the full length protein and the truncations. The increase of misincorporation frequency of dA and dT under the BPDE-dG template is emphasized when removal of the first 1-21aa in the N-terminus of mPolκ (Table II). Lior-Hoffmann *et al.* (*37*) using molecular modelling and dynamic simulations, show that a hydrogen bond forms between the BP residue and Met135 in the full length Polκ, hence a misincorporation of dTTP is less feasible, as demonstrated in previous work (*20*–*22*) and in Table II. When removal of the first 21 residues in mPolκ, we suspect that the changes in Polκ structural integrity and flexibility may permit the adducted template base G* to position itself optimally for wobble pair geometry with dTTP, as we see 5- and 8-fold increase in misincorporation frequencies of dTTP opposite BPDE-dG compared with that of the Polκ$_{1\text{-}852}$ and Polκ$_{1\text{-}516}$, respectively (Table II).

Studies by Lone *et al.* (*17*) have shown that the first 18 N-terminal amino acids of hPolκ played important role in mismatch extension. hPolκ minus the first 18 residues has severely diminished ability to extend mismatched primer template termini, while it retains primer extension proficiency from matched termini (*17*). On the undamaged DNA template, we found that Polκ$_{22\text{-}516}$ retains similar proficiency for insertion correct dCTP and a lower efficiency for misincorporation opposite normal G (Table I), compared with that of full length Polκ. These observations confirmed the conclusion by Lone *et al.* (*17*) that the first 18 N-terminal residues contribute additionally to the misinsertion efficiency. In the case of BPDE-modified dG DNA, we found that compared with full-length protein, mPolκ missing the first 21 residues exhibited greatly reduced ability in the translesion synthesis of the BPDE-dG lesion (Fig. 2D, Table II), and the fidelity of the nucleotide incorporation opposite the lesion was reduced due to the deletions (Table II), suggesting that the amino acids of the Polκ N-terminal region contribute to its TLS ability independent of DNA lesions.

Together, through biochemical comparison of these Polκ truncated forms with the full length mPolκ, we have found that deletion of the first 21 residues in mPolκ severely impairs its efficiency and accuracy in bypass of the BPDE-DNA. The stalling of Polκ$_{22\text{-}516}$ reflects not only on the nucleotide incorporation step but also on primer extension immediately after the lesion. Hence, an intact N-terminus part is necessary for Polκ to fulfill its optimal TLS functions opposite BPDE-dG lesions.

Supplementary Data

Supplementary Data are available at *JB* Online.

Acknowledgements

We are grateful to Prof. Nicholas Geacintov for providing the 11-nt BPDE-modified strand, and Dr Wei Yang for helpful discussions about the project.

Funding
This work was supported by the National Natural Science Foundation of China (Grant nos: 31300658, 31470784, 31170730, 31471331) and the Strategic Priority Research Program of the Chinese Academy of Sciences (XDB14030302).

Conflict of Interest
None declared.

References

1. Friedberg, E., Walker, G., Siede, W., Wood, R., Schultz, R., and Ellenberger, T. (2006) DNA Repair and Mutagenesis, 2nd edn. ASM Press, Washington, DC
2. Ohmori, H., Friedberg, E. C., Fuchs, R. P., Goodman, M. F., Hanaoka, F., Hinkle, D., Kunkel, T. A., Lawrence, C. W., Livneh, Z., Nohmi, T., Prakash, L., Prakash, S., Todo, T., Walker, G. C., Wang, Z., and Woodgate, R. (2001) The Y-family of DNA polymerases. *Mol. Cell* **8**, 7–8
3. Yang, W. (2003) Damage repair DNA polymerases Y. *Curr. Opin. Struct. Biol.* **13**, 23–30
4. Lange, S. S., Takata, K., and Wood, R. D. (2011) DNA polymerases and cancer. *Nat. Rev. Cancer* **11**, 96–110
5. Yang, W. (2014) An Overview of Y-Family DNA Polymerases and a Case Study of Human DNA Polymerase eta. *Biochemistry* **53**, 2793–2803.
6. Johnson, R. E., Prakash, S., and Prakash, L. (1999) Efficient bypass of a thymine-thymine dimer by yeast DNA polymerase, Poleta. *Science* **283**, 1001–1004
7. Masutani, C., Kusumoto, R., Iwai, S., and Hanaoka, F. (2000) Mechanisms of accurate translesion synthesis by human DNA polymerase eta. *EMBO J* **19**, 3100–3109
8. Biertumpfel, C., Zhao, Y., Kondo, Y., Ramon-Maiques, S., Gregory, M., Lee, J. Y., Masutani, C., Lehmann, A. R., Hanaoka, F., and Yang, W. (2010) Structure and mechanism of human DNA polymerase eta. *Nature* **465**, 1044–1048
9. Masutani, C., Kusumoto, R., Yamada, A., Dohmae, N., Yokoi, M., Yuasa, M., Araki, M., Iwai, S., Takio, K., and Hanaoka, F. (1999) The XPV (xeroderma pigmentosum variant) gene encodes human DNA polymerase eta. *Nature* **399**, 700–704
10. Johnson, R. E., Kondratick, C. M., Prakash, S., and Prakash, L. (1999) hRAD30 mutations in the variant form of xeroderma pigmentosum. *Science* **285**, 263–265
11. Haracska, L., Johnson, R. E., Unk, I., Phillips, B. B., Hurwitz, J., Prakash, L., and Prakash, S. (2001) Targeting of human DNA polymerase iota to the replication machinery via interaction with PCNA. *Proc. Natl. Acad. Sci. U. S. A.* **98**, 14256–14261
12. Washington, M. T., Minko, I. G., Johnson, R. E., Wolfle, W. T., Harris, T. M., Lloyd, R. S., Prakash, S., and Prakash, L. (2004) Efficient and error-free replication past a minor-groove DNA adduct by the sequential action of human DNA polymerases iota and kappa. *Mol. Cell Biol.* **24**, 5687–5693
13. Choi, J. Y., Stover, J. S., Angel, K. C., Chowdhury, G., Rizzo, C. J., and Guengerich, F. P. (2006) Biochemical basis of genotoxicity of heterocyclic arylamine food mutagens: Human DNA polymerase eta selectively produces a two-base deletion in copying the N2-guanyl adduct of 2-amino-3-methylimidazo[4,5-f]quinoline but not the C8 adduct at the NarI G3 site. *J. Biol. Chem.* **281**, 25297–25306
14. Kim, J., Song, I., Jo, A., Shin, J. H., Cho, H., Eoff, R. L., Guengerich, F. P., and Choi, J. Y. (2014) Biochemical analysis of six genetic variants of error-prone human DNA polymerase iota involved in translesion DNA synthesis. *Chem. Res. Toxicol.* **27**, 1837–1852
15. Wojtaszek, J., Lee, C. J., D'Souza, S., Minesinger, B., Kim, H., D'Andrea, A. D., Walker, G. C., and Zhou, P. (2012) Structural basis of Rev1-mediated assembly of a quaternary vertebrate translesion polymerase complex consisting of Rev1, heterodimeric polymerase (Pol) zeta, and Pol kappa. *J. Biol. Chem.* **287**, 33836–33846
16. Uljon, S. N., Johnson, R. E., Edwards, T. A., Prakash, S., Prakash, L., and Aggarwal, A. K. (2004) Crystal structure of the catalytic core of human DNA polymerase kappa. *Structure* **12**, 1395–1404
17. Lone, S., Townson, S. A., Uljon, S. N., Johnson, R. E., Brahma, A., Nair, D. T., Prakash, S., Prakash, L., and Aggarwal, A. K. (2007) Human DNA polymerase kappa encircles DNA: implications for mismatch extension and lesion bypass. *Mol. Cell* **25**, 601–614
18. Cheng, S. C., Hilton, B. D., Roman, J. M., and Dipple, A. (1989) DNA adducts from carcinogenic and noncarcinogenic enantiomers of benzo[a]pyrene dihydrodiol epoxide. *Chem. Res. Toxicol.* **2**, 334–340
19. Geacintov, N. E., Cosman, M., Hingerty, B. E., Amin, S., Broyde, S., and Patel, D. J. (1997) NMR solution structures of stereoisometric covalent polycyclic aromatic carcinogen-DNA adduct: principles, patterns, and diversity. *Chem. Res. Toxicol.* **10**, 111–146
20. Zhang, Y., Wu, X., Guo, D., Rechkoblit, O., and Wang, Z. (2002) Activities of human DNA polymerase kappa in response to the major benzo[a]pyrene DNA adduct: error-free lesion bypass and extension synthesis from opposite the lesion. *DNA Repair (Amst)* **1**, 559–569
21. Rechkoblit, O., Zhang, Y., Guo, D., Wang, Z., Amin, S., Krzeminsky, J., Louneva, N., and Geacintov, N. E. (2002) trans-Lesion synthesis past bulky benzo[a]pyrene diol epoxide N2-dG and N6-dA lesions catalyzed by DNA bypass polymerases. *J. Biol. Chem.* **277**, 30488–30494
22. Huang, X., Kolbanovskiy, A., Wu, X., Zhang, Y., Wang, Z., Zhuang, P., Amin, S., and Geacintov, N. E. (2003) Effects of base sequence context on translesion synthesis past a bulky (+)-trans-anti-B[a]P-N2-dG lesion catalyzed by the Y-family polymerase pol kappa. *Biochemistry* **42**, 2456–2466
23. Liu, Y., Yang, Y., Tang, T. S., Zhang, H., Wang, Z., Friedberg, E., Yang, W., and Guo, C. (2014) Variants of mouse DNA polymerase kappa reveal a mechanism of efficient and accurate translesion synthesis past a benzo[a]pyrene dG adduct. *Proc. Natl. Acad. Sci. U. S. A.* **111**, 1789–1794
24. Ogi, T., Shinkai, Y., Tanaka, K., and Ohmori, H. (2002) Polkappa protects mammalian cells against the lethal and mutagenic effects of benzo[a]pyrene. *Proc. Natl. Acad. Sci. U. S. A.* **99**, 15548–15553
25. Avkin, S., Goldsmith, M., Velasco-Miguel, S., Geacintov, N., Friedberg, E. C., and Livneh, Z. (2004) Quantitative analysis of translesion DNA synthesis across a benzo[a]pyrene-guanine adduct in mammalian cells: the role of DNA polymerase kappa. *J. Biol. Chem.* **279**, 53298–53305
26. Bi, X., Slater, D. M., Ohmori, H., and Vaziri, C. (2005) DNA polymerase kappa is specifically required for recovery from the benzo[a]pyrene-dihydrodiol epoxide (BPDE)-induced S-phase checkpoint. *J. Biol. Chem.* **280**, 22343–22355

27. Stancel, J. N. K., McDaniel, L. D., Velasco, S., Richardson, J., Guo, C. X., and Friedberg, E. C. (2009) Polk mutant mice have a spontaneous mutator phenotype. *DNA Repair* **8**, 1355–1362
28. Mao, B., Xu, J., Li, B., Margulis, L. A., Smirnov, S., Ya, N. Q., Courtney, S. H., and Geacintov, N. E. (1995) Synthesis and characterization of covalent adducts derived from the binding of benzo[a]pyrene diol expoxide to a -GGG- sequence in a deoxyoligonucleotide. *Carcinogenesis* **16**, 357–365
29. Guo, C., Fischhaber, P. L., Luk-Paszyc, M. J., Masuda, Y., Zhou, J., Kamiya, K., Kisker, C., and Friedberg, E. C. (2003) Mouse Rev1 protein interacts with multiple DNA polymerases involved in translesion DNA synthesis. *EMBO J.* **22**, 6621–6630
30. Choi, J. Y., Angel, K. C., and Guengerich, F. P. (2006) Translesion synthesis across bulky N2-alkyl guanine DNA adducts by human DNA polymerase kappa. *J. Biol. Chem.* **281**, 21062–21072
31. Johnson, R. E., Prakash, L., and Prakash, S. (2006) Yeast and human translesion DNA synthesis polymerases: expression, purification, and biochemical characterization. *Methods Enzymol.* **408**, 390–407
32. Creighton, S., Bloom, L. B., and Goodman, M. F. (1995) Gel fidelity assay measuring nucleotide misinsertion, exonucleolytic proofreading, and lesion bypass efficiencies. *Methods Enzymol.* **262**, 232–256
33. Benkovic, S. J., and Cameron, C. E. (1995) Kinetic analysis of nucleotide incorporation and misincorporation by Klenow fragment of Escherichia coli DNA polymerase I. *Methods Enzymol.* **262**, 257–269
34. Goodman, M. F., Creighton, S., Bloom, L. B., and Petruska, J. (1993) Biochemical basis of DNA replication fidelity. *Crit. Rev. Biochem. Mol. Biol.* **28**, 83–126
35. Song, I., Kim, E. J., Kim, I. H., Park, E. M., Lee, K. E., Shin, J. H., Guengerich, F. P., and Choi, J. Y. (2014) Biochemical characterization of eight genetic variants of human DNA polymerase kappa involved in error-free bypass across bulky N-guanyl DNA adducts. *Chem. Res. Toxicol.* **27**, 919–930
36. Levine, R. L., Miller, H., Grollman, A., Ohashi, E., Ohmori, H., Masutani, C., Hanaoka, F., and Moriya, M. (2001) Translesion DNA synthesis catalyzed by human pol eta and pol kappa across 1,N6-ethenodeoxyadenosine. *J. Biol. Chem.* **276**, 18717–18721
37. Lior-Hoffmann, L., Ding, S., Geacintov, N. E., Zhang, Y., and Broyde, S. (2014) Structural and dynamic characterization of polymerase kappa's minor groove lesion processing reveals how adduct topology impacts fidelity. *Biochemistry* **53**, 5683–5691.
38. Ren, J., Wen, L., Gao, X., Jin, C., Xue, Y., and Yao, X. (2009) DOG 1.0: illustrator of protein domain structures. *Cell Res.* **19**, 271–273